Simulation of Sub-Halfmicron Mask Defect Printability at 1X Reticle Magnification

Warren W. Flack, Gary Newman, Dan Schurz
Ultratech Stepper, Inc.
San Jose, CA 95134

There has been considerable attention given to the printability of reticle defects and their impact on wafer yields. Over the last year the printability risk from small defects increased due to the wider application of Optical Proximity Correction (OPC) structures and the inclusion of more phase shifting reticles. There have been several simulation studies on the printability of sub-halfmicron defects using lens and illumination parameters of 5X reduction steppers. Since submicron 1X projection systems are being incorporated into numerous fabrication lines, there is a clear need to determine if these systems show similar sensitivity to sub-halfmicron defects as reduction steppers.

Earlier experimental work examined the printability of several classes of sub-halfmicron 25 µm defects on a submicron 1X stepper. To extend this work, a three dimensional (3D) optical lithography simulation tool has been employed to predict the printability of various reticle defect scenarios. Experimental data was used to validate the 3D simulator by comparing modeling data to SEM measurements of wafers exposed with a reticle containing programmed clear pinhole and opaque pindot defects. A statistically designed simulation study was performed to quantify the critical dimension (CD) variation resulting from defects of varying sizes, proximity to a feature edge and variations in the pitch of the impacted line/space features. An additional statistically designed simulation was then used to predict the printability behavior of defects relative to different feature sizes over a range of numerical aperture and partial coherence settings applicable to a 1X lens design. Finally, the impact of defect length and width on printability were characterized for rectangular defects over a range of sizes.

Overall, this analysis enhances the understanding of the relationship between reticle defects and 1X projection optics and allows for determination of optimal reticle defect specifications for cost effective lithography applications.

Key Words: sub-halfmicron defects, defect printability, submicron 1X steppers, defect simulation

1.0 INTRODUCTION

Considerable attention is being given to the printability of reticle defects and their impact on device yields as the semiconductor industry embraces subhalf-micron designs [1, 2, 3]. These studies typically involve 5X reticles and have shown that defect printability is dependent on defect type, size, location and stepper illumination. In general, these studies have emphasized larger defects because of the 5X reduction optics in the stepper [4]. However, as wafer lithography systems improve their resolution, small reticle defects that were previously insignificant have the potential to cause yield loss and reliability problems. The risk from small defects is heightened by the application of optical proximity correction (OPC) structures such as serifs and unresolved auxiliary patterns on reduction reticles [5]. Submicron 1X reticles and advanced 5X reticles utilizing OPC tend to have similar reticle geometries. These OPC features typically are subhalf-micron on the reticle which presents new issues for reticle manufacturing. For example, Sohn et. al. from Samsung, have reported that they expect reticle features of 0.6 μm and OPC features of 0.3 μm on 1 Gb DRAM reticle sets by the year 2000 [6].

In order to extend the productive life of existing lithography systems for smaller devices, considerable attention has been given to optimizing stepper performance by adjusting numerical aperture (NA) and partial coherence (σ) for maximum process latitude at minimum CD. It is well documented that the proximity effect of dense patterns causes CD variations across a field. Mack notes that one of the contributing factors is that the aerial image of a dense pattern is different from that of an isolated feature [7]. Because many process layers contain both isolated and dense patterns, statistical methods of optimizing the NA and σ values have been developed for "iso-dense" patterns which minimize both proximity effect and CD distribution. Miller et. al. have concluded that adjusting to mid NA and high σ values for specific layers can maximize process latitude and throughput [8].

It has been demonstrated that CD control is affected by variations in pattern pitch over an exposed field in wafer processing [9]. Earlier experimental work, in which defect printability was measured by CD variation, also suggested that defects would have different printability potential depending on the pitch of their environment [10]. A study of 0.25 μm and 0.375 μm reduction lithography by Yan et. al., which has related mask defect printability to wafer process CD distribution, was done in a pattern pitch ≥ 1.5 [2]. Since most of the layers comprising an integrated circuit consist of unequal lines and spaces, it was deemed necessary to observe defect printability through changes in pitch in the minimum design rule.

In various studies on reduction lithography, there is agreement that defect area, rather than linear size, is a determining factor in CD control [2, 10]. Yan has also determined that CD change is a linear function of defect area and that improvements in CD control will reduce the printability probability of a given mask defect [2].

Because 1X steppers with sub-micron resolution capability are increasingly used in wafer lithography, especially in mix and match applications, it becomes increasingly important to

understand any differences in pattern sensitivity to reticle defects between these lithography systems [12]. In an earlier experiment, the effects of a series of clear and opaque reticle defects were observed on wafers exposed using a 1X projection stepper [10]. Similarities were found in defect behavior pertaining to defect size, proximity to line edge and tone in both reduction systems and 1X projection systems. However, a review of the current literature confirms that other aspects of the 1X lithography system need to be explored in order to establish sound defect behavioral rules. Several of the optical parameters affecting defect printability such as illumination system and defect pattern pitch, could not be sufficiently explored under the prevailing experimental conditions. For example, the 1X lithography system used did not have controls to vary either numerical aperture (NA) or partial coherence (σ). The reticle design replicated a 64 Mb DRAM metal layer which was not applicable to observing defect behavior in a variety of line/space dimensions. Reticle defects were measured in single dimension size rather than area. Before attempting to design and build a test reticle capable of answering the many questions that have arisen from the experimental results and the literature, it was decided that a series of simulation runs could be used to narrow the purposes and the design requirements of the future reticle.

2.0 EXPERIMENTAL METHODS

2.1 Process Simulation

Optical microlithography simulation programs have been shown to provide results representative of actual production processes. Given the simulation is well matched to the true process, an extensive number of variable combinations may be easily investigated. Solid-C®, a commercially available optical lithography simulation program, was used to generate all the results presented in this work. Inputs to the simulation program remained constant for the photoresist and stepper parameters included in Tables 1a and 1b.

Matching lithography simulation to experimental results has been investigated in other works [15]. One matching procedure involves comparison of simulated and actual swing curves. Thorton and Mack determined that adjustments could be made to the photoresist **C** parameter and photoresist index of refraction to match the swing curves. These adjustments are employed to compensate for differences in relative photoresist thickness measurements and exposure dose calibration differences.

A different matching approach was performed in this study. An experimental focus/exposure matrix was generated from which a Bossung plot was generated. The plot of the process window was then compared to simulated results generated with many of the parameters included in Tables 1a and 1b. Both the experimental and simulated Bossung plots are shown in Figures 2 and 3 respectively. For the experimental data, to determine the process window on a Ultratech Saturn

Wafer Stepper® the exposure was varied from 155 to 215 mJ/cm^2, and focus was varied from -2 to +2 µm, . The nominal exposure conditions were determined by exposing a wafer and measuring the desired CD on a Hitachi S-7280 SEM. Nominal exposure dose was determined to be 170 mJ/cm^2 with an optimal defocus setting of 0 µm.

The experimental and modeled plots are very similar other than an offset in nominal exposure energy of approximately 25 mJ/cm^2. Both plots indicate approximately 2µm of focus latitude and 30 mJ/cm^2 of exposure latitude. The relative difference in exposure energy may be accounted for by slight differences in the simulated and actual optical parameters of the lithography system. For example, the Saturn optical system contains a designed central obscuration which was not accounted for in the simulation. Additionally, the exposure illumination contains wavelengths from 355 to 375 nm and the continuum. The simulated process window was generated using monochromatic i-line illumination. In addition, differences in the photoresist development process could result in small changes in the parameters of the Mack development model.

2.2 Statistically Designed Experiment

Simulation experiments were designed to allow for the observation of defect behavior in several optical system and pattern conditions. Because previous studies have shown that defect area has a greater influence on printability than defect size and shape, a variety of defect sizes at several aspect ratios are incorporated in the simulation exercises. A series of width to length ratios, ranging from 1:1 to 1:2.5 µm was used to validate the assumption that defect area would have the same linear influence on CDs in the 1X projection system as had been noted in the work on reduction systems.

The results of this experiment were sufficient grounds for the speculation that defect sizes in the 0.20 to 0.35 µm range had the potential to cause CD variations exceeding 10 percent in a 0.65 µm line/space pattern which is similar to the design rule for the non-critical layers of a 64Mb DRAM. However, more data is required in order to attempt a prediction of defect behavior within this design rule.

Three combinations of optical imaging system parameters, defect characteristics and their corresponding effect on printability were investigated in this study and are included in Table 2. Each of these combinations were investigated in both opaque and clear pinhole defects. In cases where imaging system parameters were held constant, an Ultratech Saturn Wafer Stepper was simulated. The Ultratech stepper is based on the 1X Wynne-Dyson lens design employing broadband i-line illumination from 355 to 375 nm [13]. The Ultratech Saturn has a numerical aperture (NA) of 0.365 and is specified at 0.65 µm resolution with 1.5 µm depth of focus (DOF) and a field size of 44 x 22 mm.

To effectively characterize the variable combinations included in Table 2, a statistically designed experiment (SDE) was used. JMP®, a commercially available statistics program from SAS Institute, was used to generate the n-dimensional design space and perform the analysis of

variance. A higher order experimental design was selected to provide a response surface which incorporates linear and nonlinear factor effects as well as interactions. Potential design schemes included a three level factorial, Box-Behnken, central composite and quadratic designs [14]. The Box-Behnken was selected since it is the most efficient design requiring only 13 unique trails for three factors. The geometric character of the Box-Behnken design is a hypercube with experimental trials located at midpoint factor levels. However, because of this midpoint approach the design suffers potential model errors at the corners of the design space. The final design space was reviewed to insure that all variable combinations were physically valid. When necessary, unattainable conditions were removed from the designed experiment and replaced with boundary conditions. The response to each of the combinations is defined as the change in the normalized CD printing in the photoresist.

The imaging system parameters examined are those typically applicable to a 1X lens design. The range of defect characteristics investigated are taken from an earlier study [10]. The range of variables investigated for three SDEs are included in Table 3.

3.0 RESULTS AND DISCUSSIONS

3.1 Pitch and Proximity

The first SDE was performed to analyze the effects of three factors on the printability of reticle defects on a Saturn Stepper: line/space pitch, defect proximity to the edge of the pitch structure and the size of the defects. For this case the defects are assumed to have a square aspect ratio. Rectangular defects with varying ratios of length to width will be discussed in section 3.2.

Since the defect sizes selected are all below the really minimum controllable resolution of the Saturn Stepper, the response was defined as the change in the normalized CD printing in the photoresist. For an opaque defect this corresponds to the measured space size divided by the drawn space size. For a clear pinhole defect the normalized CD corresponds to the measured line size divided by the drawn line size. A 50 percent threshold criteria was selected for the measured CD since this is the specification frequently used in wafer metrology equipment.

A total of 13 simulation trials were performed for each SDE as described in section 2.2. This Box-Behnken design provides sufficient statistical degrees of freedom for the extraction of the main effects and two-way interactions [14]. An analysis of variance was performed using JMP® software [16]. The results for opaque defects are shown in Table 4. The estimate is the model coefficient determined by least squares analysis. The sum of squares (Sum of Sq) is the sum of the squares of the difference between the fitted response and the actual response. The F Ratio is the F statistic for testing that the regression factor is zero. Finally the Prob>F is the probability of obtaining a greater F value by chance alone. For this study significance probabilities of 0.10 or less are considered evidence that the regression factor is significant (90 percent confidence level).

It is apparent that only defect size and pitch*defect size factors are significant using this test criteria. While the proximity as a factor is insignificant, the cross terms of pitch*proximity and defect size*proximity are much more significant. For the total model the R^2 adjusted for the degrees of freedom is 0.818. An R^2 of 1 occurs when there is a perfect fit between the actual and predicted response.

Contour plots of line/space pitch versus defect size, and defect proximity versus defect size are shown in Figures 4(a) and 4(b) respectively. Note that in each plot the third factor is held constant as labeled. Figure 4(a) shows that the impact on normalized CD increases rapidly as the defect size increases and the pitch decreases. However, for a pitch larger than about 2 µm the impact on CD control is less than 10 percent for the entire range of defect sizes. Figure 4(b) shows that the impact on normalized CD increases moderately as the defect size increases and defect proximity decreases. It is clear from these figures that line/space pitch is a stronger influence on defect printability than defect proximity.

This SDE was repeated for clear pinhole defects as shown in Table 5. For this case the factors of defect size, proximity and pitch*proximity were determined to be significant with a 90 percent confidence level. For clear pinhole defects, the proximity is more of a significant factor than for opaque defects. This is probably due to the observation that opaque defects tend to print at smaller sizes than clear pinhole defects [8]. For the total model the adjusted R^2 is 0.891. This indicates a better model fit than that obtained for the opaque defects.

Contour plots of line/space pitch versus defect size, and defect proximity versus defect size are shown in Figures 5(a) and 5(b) respectively. Again, for each plot the third factor is held constant as labeled. Figure 5(a) shows a much stronger effect of pitch for smaller defects than was observed for the opaque defect case. There is also much less curvature to the contour lines which probably explains why the adjusted R^2 fit is better for the clear pinhole defects. Figure 5(b) also shows a much stronger dependency on proximity for small clear pinhole defects than was observed for opaque defects. However, overall the same trend is observed that line/space pitch is a stronger influence on defect printability than defect proximity.

3.2 Length to Width Defect Ratio

The next SDE was performed to analyze the effects of two factors on the printability of reticle defects on a Saturn Stepper: the aspect ratio of a rectangular defect (length to width ratio) and the size (width) of the defects. For this case the pitch is held constant at 1.3 µm and the defects are placed at the edge of the line/space structure (proximity equals zero). The results for opaque defects are shown in Table 6. It is apparent that the three factors of defect size, defect ratio and defect size*ratio are significant with a 90 percent confidence level. Since these factors all describe physical attributes of the defect, it is reasonable to expect similar levels of significance. For opaque defects the adjusted R^2 of the total model is 0.915. The results for clear pinhole defects are shown in Table 7. The two factors of defect ratio and defect size*ratio are significant with a 90

percent confidence level. As in the previous section on pitch and proximity, the clear pinhole defects show less sensitivity to defect size. For clear pinhole defects the adjusted R^2 of the total model is 0.989.

Contour plots of the aspect ratio (length to width) versus defect size (width) for opaque and clear pinhole defects are shown in Figures 6(a) and 6(b) respectively. For both cases the normalized CD decreases rapidly with increasing defect size and defect aspect ratio. However, for small defects the opaque case shows substantially less sensitivity to defect aspect ratio. In contrast, the clear pinhole case shows an overall lower sensitivity to defect printability than the opaque case. For example at a defect size of 0.3 μm and an aspect ratio of 2.0, the normalized CD is 0.4 and 0.55 for the opaque and clear pinhole cases respectively. Once again there is less curvature to the contour lines for the clear pinhole case which probably explains why the adjusted R^2 fit is better than for the opaque defects.

3.3 Numerical Aperture and Partial Coherence

The third SDE was performed to analyze the effects of three factors on the printability of reticle defects on a generic stepper: lens numerical aperture, lens partial coherence and the size of the defects. For this case the defects are assumed to have a square aspect ratio. The pitch is held constant at 1.3 μm and the defects are placed at the edge of the line/space structure (proximity equals zero). The results for opaque defects are shown in Table 8. It is apparent that only defect size, numerical aperture and defect size* numerical aperture factors are significant with a 90 percent confidence level. Neither the partial coherence or any cross term containing partial coherence is significant. For the total model the adjusted R^2 is 0.618. This is a fairly poor fit of the data which suggests that this model does not adequately describe the results.

Contour plots of numerical aperture versus defect size and partial coherence versus defect size are shown in Figures 7(a) and 7(b) respectively. Note that in each plot the third factor is held constant as labeled. Figure 7(a) shows that the impact on normalized CD increases rapidly as the defect size increases and the numerical aperture decreases. However, for small defects there is minimal impact of numerical aperture on defect printability. Figure 7(b) shows that partial coherence has almost no impact on normalized CD, which agrees with the analysis of variation described in Table 8.

This SDE was repeated for clear pinhole defects as shown in Table 9. For this case none of the factors appear to be significant with a 90 percent confidence level. However a forward stepwise regression analysis did establish that defect size is significant and produces an adjusted R^2 of 0.79. For the total model in Table 9 the adjusted R^2 is 0.803. Thus the improvement in the model from adding the additional factors of NA and σ is extremely small. Regardless, the clear pinhole produces a better model fit than that obtained for the opaque defects.

Contour plots of numerical aperture versus defect size and partial coherence versus defect size are shown in Figures 8(a) and 8(b) respectively. Note that in each plot the third factor is held constant

as labeled. The figures clearly show that numerical aperture and partial coherence have almost no impact on the normalized CD. The dominant factor is the defect size. There is also much less curvature to the contour lines for the numerical aperture case, which probably explains why the adjusted R^2 fit is better for the clear pinhole defects.

4.0 CONCLUSIONS

A three dimensional optical lithography simulation tool has been employed to predict the printability of various reticle defect scenarios. Experimental data was used to validate the 3D simulator by comparing modeling data to SEM measurements of wafers exposed with a reticle containing programmed clear pinhole and opaque pindot defects.

A statistically designed simulation study was performed to quantify the critical dimension (CD) variation resulting from defects of varying sizes, proximity to a feature edge and variations in the pitch of the impacted line/space features. It was observed that defect size and pitch are the dominant factors. However, for clear pinhole defects proximity is a more significant factor than for opaque defects.

A second SDE evaluated the impact of defect length and width on printability, characterized for rectangular defects over a range of sizes. The defect ratio and defect size*defect ratio were found to be significant for both opaque and clear pindot defects. However, for small defects the opaque case shows substantially less sensitivity to defect aspect ratio. In contrast, the clear pinhole case shows an overall lower sensitivity to defect printability than the opaque case.

A final SDE was then used to predict the printability behavior of defects relative to different feature sizes over a range of numerical aperture and partial coherence settings applicable to a 1X lens design. Only defect size, numerical aperture and their cross product were found to be significant factors. However, the adjusted R^2 for the opaque defect was low, which indicates that this simple model does not adequately describe the results.

5.0 REFERENCES

1. B. J. Grenon, K. D. Badger, M. J. Trybendis, “Reticle Defect Sizing and Printability,” *Symposium on Photomask Technology and Management Proceedings*, SPIE **1604** (1991).

2. P. Yan, J. Langston, J. Neff, R. Chatterjee, “Mask Defect Printability and Wafer Process Critical Dimension Control at 0.25 µm Design Rules,” *Bacus News*, **12** (1) Jan 1996.

3. T. Kikuchi et.al., “Effects of Subhalf-Micron Defects on Wafer Images During VLSI Circuit Production,” *Optical/Laser Microlithography II Proceedings*, SPIE **1088** (1989).

4. J. N. Wiley, J. A. Reynolds, “Device Yield and Reliability by Specification of Mask Defects,” *Solid State Technology*, **36**(7), July 1993.

5. M. Rieger, J. Stirniman, “Customizing Proximity Correction for Process-Specific Objectives,” *Optical Microlithography IX Proceedings*, SPIE **2726** (1996).

6. J. Sohn, S. Choi, B. Kim, H. Cho and H. Yoon, “Mask Technology for 0.18 Micron Device Generation,” *Bacus News*, **12**(7) July 1996.

7. C. Mack, “Reducing Proximity Effects in Optical Lithography,” *Microlithography Seminar Interface ‘96 Proceedings*, Olin Microelectronic Materials (1996).

8. S. Miller et. al., “Getting the Most from i-line Technology by Optimizing Numerical Aperture and Partial Coherence for Critical Layers,” *Microlithography Seminar Interface ‘96 Proceedings*, Olin Microelectronic Materials (1996).

9. C. Progler and W. Krisa, “Understanding the Effect of Pitch on Linewidth Control,” *Microlithography Seminar Interface ‘96 Proceedings*, Olin Microelectronic Materials (1996).

10. D. Schurz, W. Flack and G. Newman, “Sub-Micron Mask Defect Detectability and Printability at 1X Reticle Magnification,” *Symposium on Photomask Technology and Management Proceedings*, SPIE **2884** (1996).

11. L. Karklin, “A Comprehensive Simulation Study of the Photomask Defects Printability,” *Symposium on Photomask Technology and Management Proceedings*, SPIE **2621** (1995).

12. G. Flores, W. Flack and J. Cossins, “The Implementation and Characterization of Advanced Mix-and-Match Lithography,” *Environmental Productivity and Defect Issues in Semiconductor Manufacturing Proceedings*, SEMICON/Europa Technical Conference (1994).

13. R. Hershel, “Characterization of the Ultratech Wafer Stepper,” *Optical Microlithography Proceedings*, SPIE **334** (1982).

14. G. Box, W. Hunter and J. Hunter, *Statistics for Experimenters*, Wiley Interscience, John Wiley and Sons, New York (1978).

15. S. Thorton and C. Mack, “Lithography Modeling Tuning,” *Optical Microlithography IX Proceedings*, SPIE **2726** (1996).

16. JMP® Reference Manual, SAS Institute Inc. (1994).

Parameter	Value
Photoresist softbake temperature (^{o}C)	90
Photoresist bake time (seconds)	30
Photoresist thickness (μm)	0.98
Photoresist A parameter (μm^{-1})	0.5506
Photoresist B parameter (μm^{-1})	0.0656
Photoresist C parameter (cm^2/mJ)	0.0141
Photoresist index of refraction	1.7
Substrate type	Bare silicon
PEB diffusion length (μm)	0.065
PEB thickness loss (μm)	0
Maximum develop rate (nm/s): R_{max}	85
Minimum develop rate (nm/s): R_{min}	0.0091
Developer selectivity: n	5.8
Theshold PAC concentration: m	0.06
Develop time (seconds)	60

Table 1a: Constant Simulation Input Parameters for the substrate and photoresist processing.

Parameter	Value
Reduction factor	1X
Wavelength (nm)	365
Exposure Energy (mJ/cm^2)	200
Defocus setting (μm)	0

Table 1b: Constant Simulation Input Parameters for the lithography system.

SDE Number	Parameters Investigated
1	Defect Size, Defect Proximity to an adjacent feature, and line/space pitch
2	Defect Size and Defect aspect ratio (length/width)
3	Partial Coherence, Numerical Aperture

Table 2: Variable combinations investigated for each statistically designed experiment.

Parameter	Range Investigated
Box-Behnken Design #1	
Defect Size (µm)	0.2 to 0.35
Defect Proximity to adjacent feature (µm)	0.15 to 0.45
Pitch of adjacent feature (µm)	1.0 to 2.5
Box-Behnken Design #2	
Defect Size (µm)	0.2 to 0.35
Defect Aspect Ratio (length/width)	1 to 2.5
Box-Behnken Design #3	
Numerical Aperture	0.3 to 0.6
Partial Coherence	0.3 to 0.7
Defect Size (µm)	0.2 to 0.35

Table 3: Range of variables investigated for the three Box-Behnken designs.

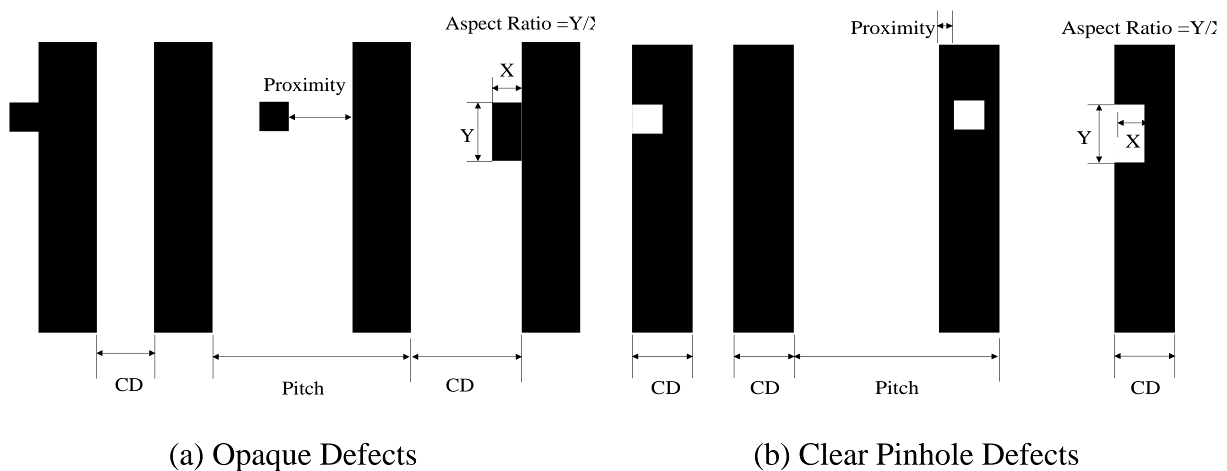

Figure 1: Illustration of pitch, proximity, and aspect ratio for opaque and clear defects.

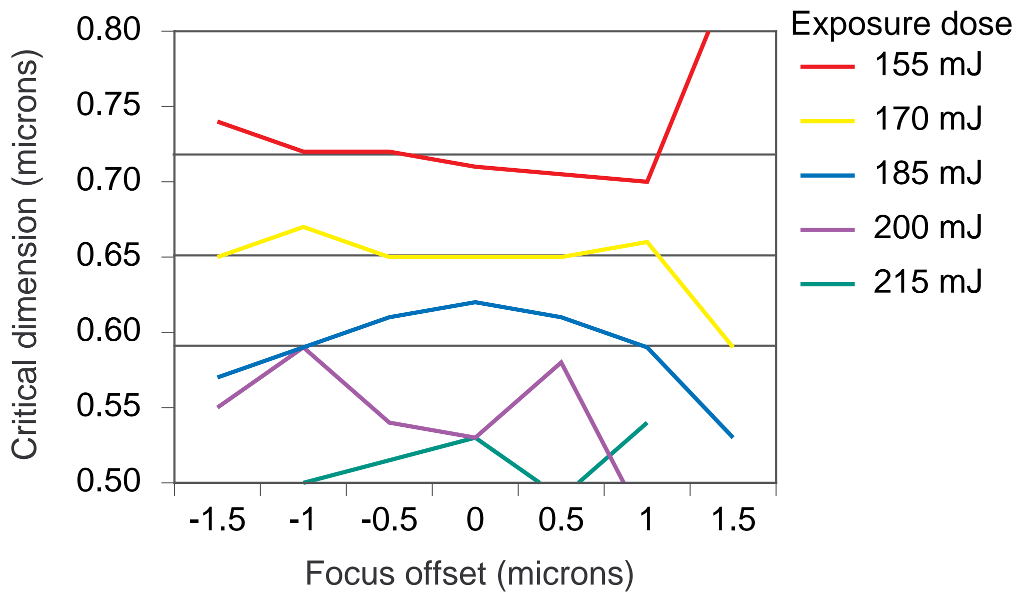

Figure 2: Experimental Bossung Plot on an Ultratech Saturn Stepper.

\

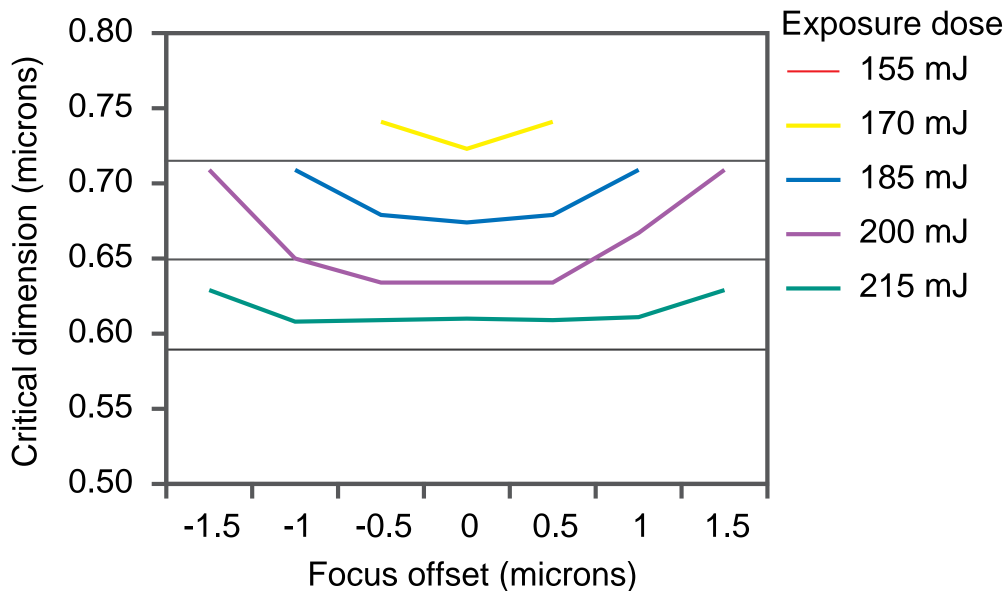

Figure 3: Simulated Bossung Plot under the same conditions as Figure 2.

Factors	Estimate	Sum of Sq	F Ratio	Prob>F
Pitch	-0.109	0.000789	0.279	0.6165
Defect Size	-4.607	0.047924	16.93	0.0063
Proximity	0.652	0.001088	0.384	0.5582
Pitch*Defect Size	1.429	0.013698	4.838	0.0701
Pitch*Proximity	-0.666	0.008901	3.144	0.1266
Defect Size*Proximity	3.503	0.005323	1.880	0.2194

Table 4: Regression analysis of the effect of pitch, defect size and proximity on normalized critical dimension control for opaque defects. The summary of fit for R^2 is 0.909 and adjusted for degrees of freedom R^2 is 0.818.

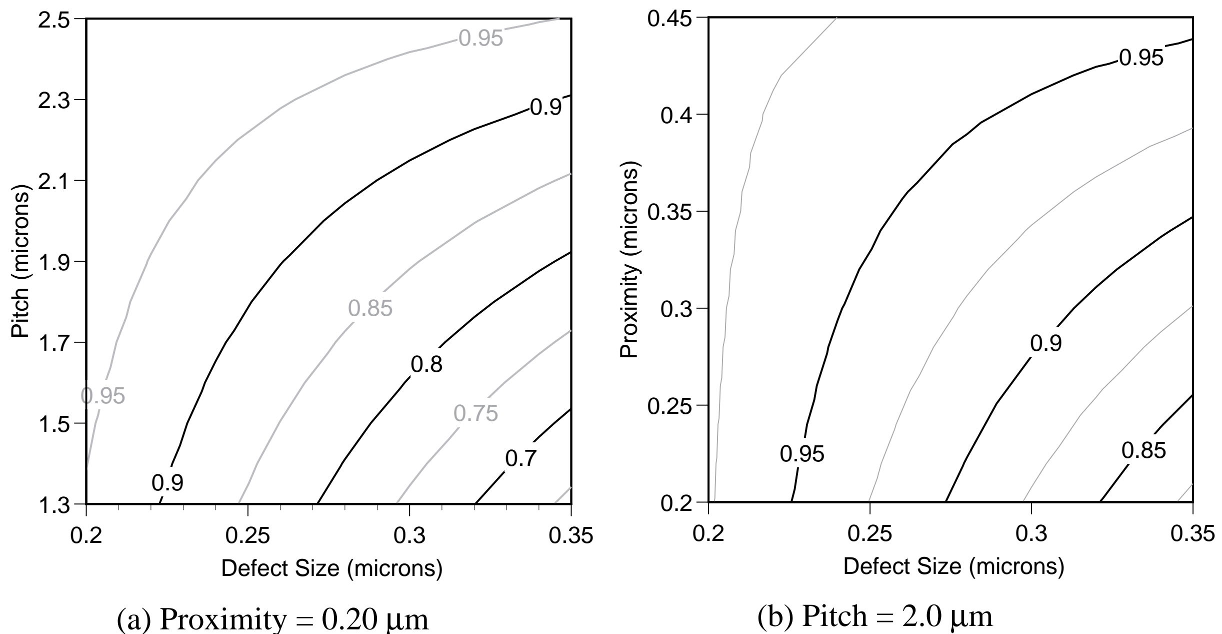

(a) Proximity = 0.20 μm

(b) Pitch = 2.0 μm

Figure 4(a): Plot of line pitch versus opaque defect size for a fixed defect proximity to the line edge. **Figure 4(b):** Plot of defect proximity versus opaque defect size for a fixed pitch. The response is the normalized critical dimension where a value of 1 indicates no impact on line/space width.

Factors	Estimate	Sum of Sq	F Ratio	Prob>F
Pitch	-0.170	0.001921	1.662	0.2448
Defect Size	-2.129	0.010236	8.853	0.0248
Proximity	1.420	0.005154	4.458	0.0792
Pitch*Defect Size	0.590	0.002330	2.015	0.2055
Pitch*Proximity	-0.834	0.013943	12.06	0.0133
Defect Size*Proximity	2.099	0.001911	1.653	0.2459

Table 5: Regression analysis of the effect of pitch, defect size and proximity on normalized critical dimension control for clear pinhole defects.The summary of fit for R^2 is 0.946 and adjusted for degrees of freedom R^2 is 0.891.

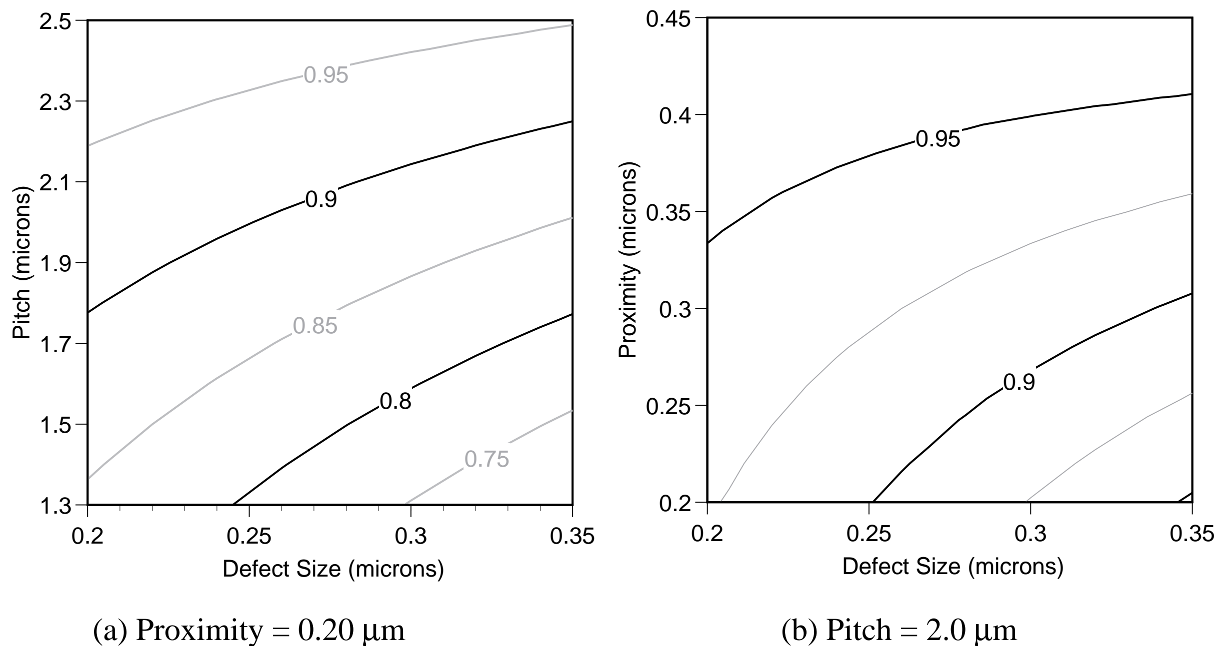

(a) Proximity = 0.20 µm

(b) Pitch = 2.0 µm

Figure 5(a): Plot of line pitch versus clear pinhole defect size for a fixed defect proximity to the space edge. **Figure 5(b):** Plot of defect proximity versus clear pinhole defect size for a fixed pitch. The response is the normalized critical dimension where a value of 1 indicates no impact on line/space width.

Factors	Estimate	Sum of Sq	F Ratio	Prob>F
Defect Size (W)	3.2440	0.025326	4.715	0.0526
Defect Ratio (L/W)	0.8005	0.072408	13.48	0.0037
Defect Size *Ratio	-4.297	0.133870	24.92	0.0004

Table 6: Regression analysis of the effect of defect size (width), defect ratio (length/width) on normalized critical dimension control for opaque defects.The summary of fit for R^2 is 0.934 and adjusted for degrees of freedom R^2 is 0.915.

Factors	Estimate	Sum of Sq	F Ratio	Prob>F
Defect Size (W)	-0.4204	0.000425	2.695	0.129
Defect Ratio (L/W)	0.1179	0.001569	9.945	0.0092
Defect Size*Ratio	-1.0133	0.007444	47.16	<0.0001

Table 7: Regression analysis of the effect of defect size (width), defect ratio (length/width) on normalized critical dimension control for clear pinhole defects.The summary of fit for R^2 is 0.991 and adjusted for degrees of freedom R^2 is 0.989.

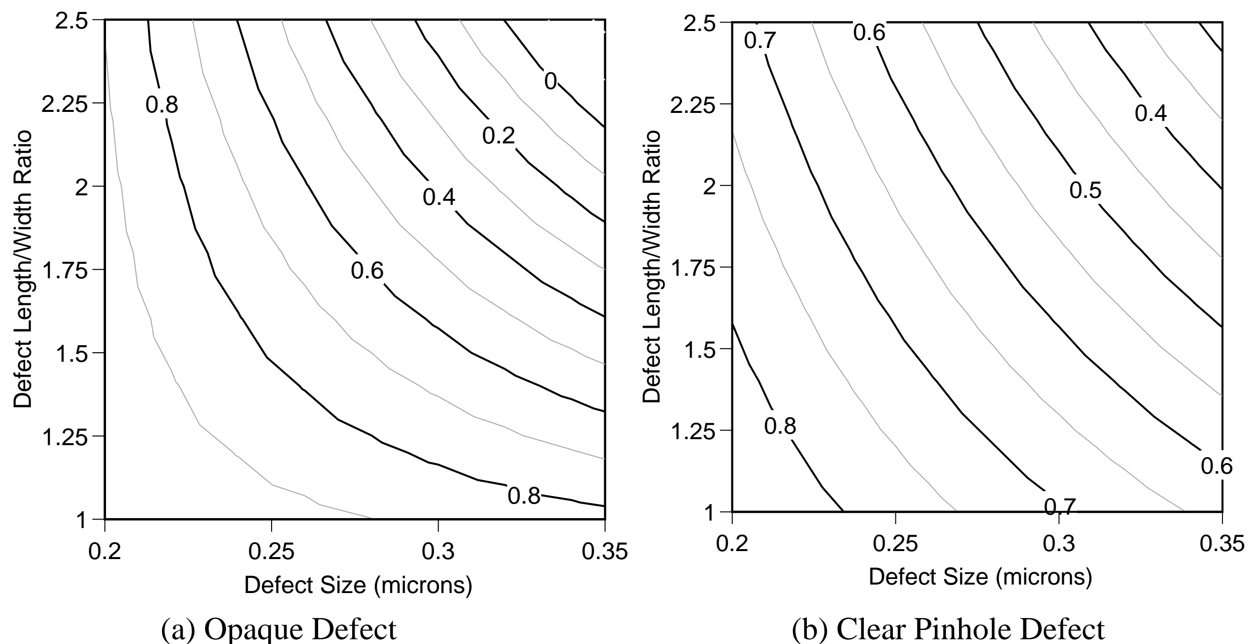

Figure 6(a): Plot of defect length/width ratio versus opaque defect size. **Figure 6(b):** Plot of defect length/width ratio versus clear pinhole defect size. The response is the normalized critical dimension where a value of 1 indicates no impact on line/space width.

Factors	Estimate	Sum of Sq	F Ratio	Prob>F
Defect Size	-6.6154	0.043416	4.020	0.0918
Numerical Aperture (NA)	-3.3308	0.040937	3.791	0.0995
Partial Coherence (Sigma)	-0.2558	0.000386	0.0357	0.8563
Defect Size*NA	11.077	0.043136	3.995	0.0926
Defect Size*Sigma	-1.8461	0.002130	0.1973	0.6725
NA*Sigma	1.4103	0.007160	0.6630	0.4466

Table 8: Regression analysis of the effect of defect size, numerical aperture and partial coherence on normalized critical dimension control for opaque defects.The summary of fit for R^2 is 0.809 and adjusted for degrees of freedom R^2 is 0.618.

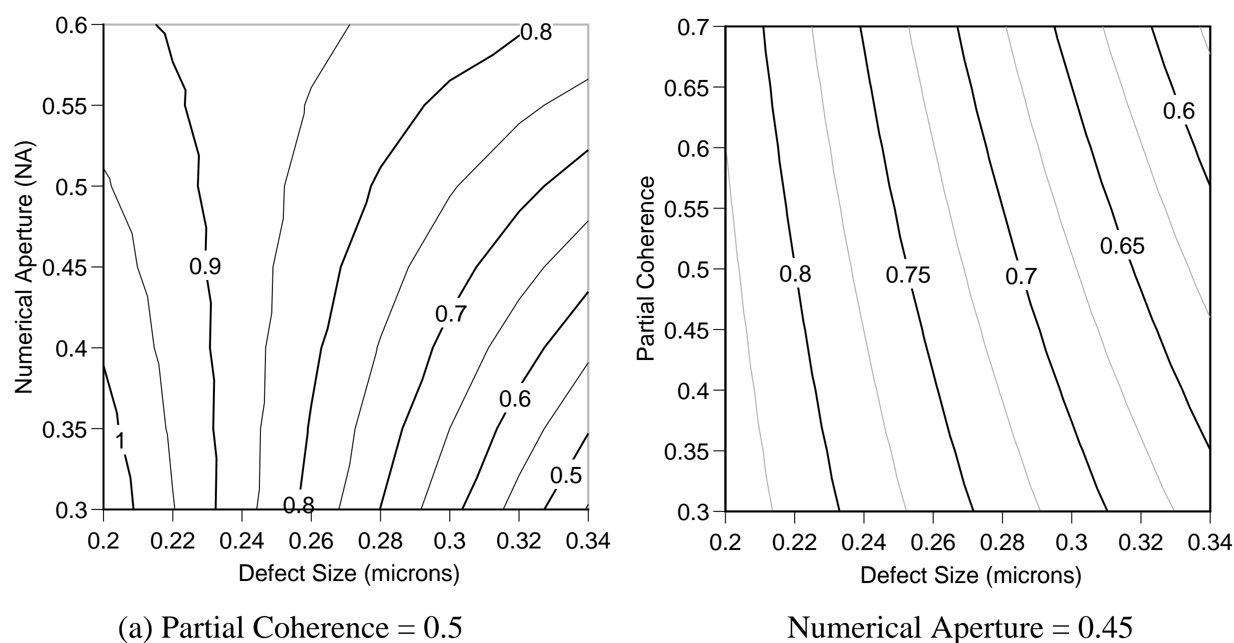

Figure 7(a): Plot of numerical aperture versus opaque defect size for a fixed partial coherence.
Figure 7(b): Plot of partial coherence versus opaque defect size for a fixed numerical aperture. The response is the normalized critical dimension where a value of 1 indicates no impact on line/space width.

Factors	Estimate	Sum of Sq	F Ratio	Prob>F
Defect Size	-0.5538	0.000304	0.199	0.6713
Numerical Aperture (NA)	0.5231	0.001009	0.660	0.4477
Partial Coherence (Sigma)	0.5346	0.001685	1.101	0.3345
Defect Size*NA	-0.8205	0.000237	0.155	0.7078
Defect Size*Sigma	-1.231	0.000947	0.618	0.4616
NA*Sigma	-0.7692	0.002130	1.392	0.2828

Table 9: Regression analysis of the effect of defect size, numerical aperture and partial coherence on normalized critical dimension control for clear pinhole defects.The summary of fit for R^2 is 0.902 and adjusted for degrees of freedom R^2 is 0.803.

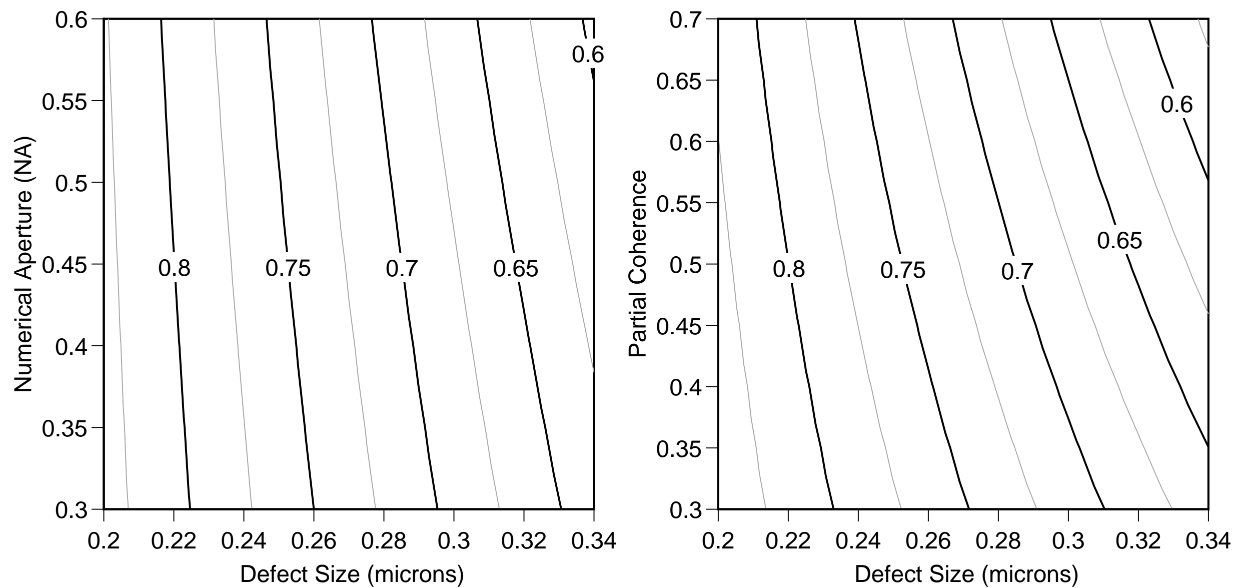

(a) Partial Coherence = 0.5

(b) Numerical Aperture = 0.45

Figure 8(a): Plot of numerical aperture versus clear pinhole defect size for a fixed partial coherence. **Figure 8(b):** Plot of partial coherence versus clear pinhole defect size for a fixed numerical aperture. The response is the normalized critical dimension where a value of 1 indicates no impact on line/space width.